

A Tetrameric Cage with  $D_{2h}$  Symmetry through Alkyne Metathesis\*\*

Qi Wang, Chenxi Zhang, Bruce C. Noll, Hai Long, Yinghua Jin, and Wei Zhang\*

**Abstract:** Shape-persistent covalent organic polyhedrons (COPs) with ethynylene linkers are usually prepared through kinetically controlled cross-coupling reactions. The high-yielding synthesis of ethynylene-linked rigid tetrameric cages via one-step alkyne metathesis from readily accessible triyne precursors is presented. The tetrameric cage contains two macrocyclic panels and exhibits  $D_{2h}$  symmetry. The assembly of such a COP is a thermodynamically controlled process, which involves the initial formation of macrocycles as key intermediates followed by the connection of two macrocycles with ethynylene linkages. With a large internal cavity, the cage exhibits a high binding selectivity toward  $C_{70}$  ( $K=3.9 \times 10^3 \text{ L mol}^{-1}$ ) over  $C_{60}$  (no noticeable binding).

In recent years, discrete purely organic cage molecules, that is, covalent organic polyhedrons (COPs), have attracted great attention owing to their unique properties and interesting applications in gas adsorption/separation,<sup>[1–3]</sup> host–guest recognition,<sup>[4–6]</sup> and as molecular “flasks”.<sup>[7,8]</sup> Moreover, their great potential in emerging applications such as catalysis and drug delivery is highly attractive. Recent advances in dynamic covalent chemistry (DC<sub>v</sub>C) have provided powerful thermodynamically controlled approaches towards COPs.<sup>[9–13]</sup> Most COPs reported to date are assembled through dynamic imine chemistry or boronic acid condensation.<sup>[11,14–16]</sup> Although these COPs have shown intriguing applications in chemistry and materials science, imine or B–O linkages are susceptible to hydrolysis in the presence of acid, base, or even moisture,<sup>[17,18]</sup> which leads to the decomposition of COPs and is a potential drawback for certain applications. In this regard, COPs with more robust ethynylene linkages have attracted our attention. Besides the rigidity and high chemical and

thermal stability, ethynylene linkages can enable electron conjugation if needed, which would be a valuable feature for electrical, optical, and sensing applications. To date, ethynylene-linked COPs have generally been prepared through Sonogashira or Glaser-type coupling.<sup>[19–23]</sup> As coupling reactions are kinetically controlled, the target molecular cages are oftentimes obtained in low yields along with a large amount of oligomeric or polymeric side products. High-dilution (or pseudo high-dilution) conditions with a large excess of catalysts are usually applied to minimize the “over-shooting” problem, however with limited success. Alternatively, templates have been used to preorganize the monomers and direct the syntheses of nanorings, rotaxanes, or catenanes.<sup>[24–26]</sup> Herein, we report the template-free, dynamic covalent assembly of a purely hydrocarbon molecular cage through one-step alkyne metathesis. The tetrameric cage consists of two macrocyclic panels and exhibits an uncommon  $D_{2h}$  symmetry. With a large internal cavity, the cage molecule serves as a fullerene receptor and shows a high binding selectivity for  $C_{70}$  over  $C_{60}$ .

Alkyne metathesis<sup>[27–35]</sup> has emerged as an alternative viable dynamic covalent reaction. It has been widely practiced in the synthesis of natural products,<sup>[28,36]</sup> shape-persistent macrocycles,<sup>[37]</sup> and polymers.<sup>[38–40]</sup> However, alkyne metathesis has only recently been applied to more challenging COP synthesis, which involves innumerable possible oligomeric and polymeric intermediates along the pathway to the target COP. In 2011, we reported the first application of dynamic alkyne metathesis in the synthesis of an ethynylene-linked shape-persistent rectangular prism.<sup>[6]</sup> In our previous study, a (benzoyldiphenyl)acetylene moiety had to be installed in the monomer unit to drive the equilibrium to the cage product by precipitation of bis(benzoylbiphenyl)acetylene byproducts. However, installation of the precipitating groups in the monomer requires additional synthetic steps, and their poor solubility causes difficult monomer purification and premature precipitation of oligomeric intermediates. Recently, we have developed triphenolsilane-based alkyne metathesis catalysts that are compatible with 5 Å molecular sieves, which act as scavengers of small alkyne byproducts, for example 2-butyne.<sup>[41]</sup> In the presence of molecular sieves, simple propynyl-substituted monomers can undergo alkyne metathesis with high conversion in a closed system using triphenolsilane-based catalysts. Therefore, in this study, simple triynes **3a** and **3b** are designed as the monomers (Scheme 1a). Tetrahedron-shaped tetrameric cage **4T<sub>d</sub>** is expected to be the product, as compounds **3a** and **3b** are  $C_3$ -symmetric with an edge-to-face angle of 60°, which closely matches the edge-to-face angle of a tetrahedron (54.7°). The syntheses of **3a** and **3b** are straightforward starting from readily available acetyl benzene **1a** and **1b**.  $\text{SiCl}_4$ -catalyzed condensation reaction followed by Negishi coupling afforded

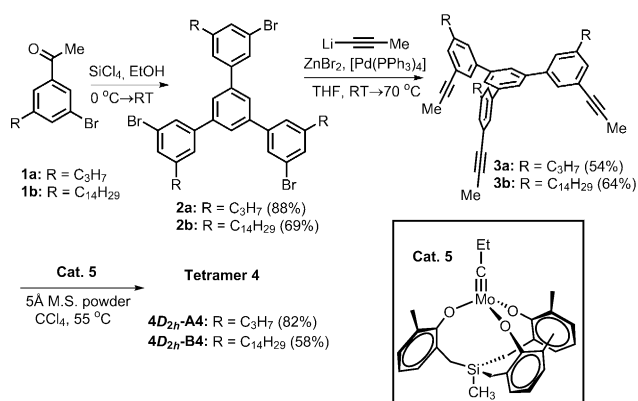
[\*] Q. Wang, C. Zhang, Dr. Y. Jin, Prof. Dr. W. Zhang  
Department of Chemistry and Biochemistry  
University of Colorado, Boulder, CO 80309 (USA)  
E-mail: wei.zhang@colorado.edu  
Homepage: <http://chem.colorado.edu/zhanggroup>

Dr. B. C. Noll  
Bruker AXS Inc.  
5465 East Cheryl Parkway, Madison, WI 53711 (USA)

Dr. H. Long  
National Renewable Energy Laboratory  
Golden, CO 80401 (USA)

[\*\*] We thank the National Science Foundation (DMR-1055705) and Alfred P. Sloan Foundation for the financial support of this research, and Youlong Zhu for helpful discussions. This research used capabilities of the National Renewable Energy Laboratory Computational Sciences Center, which is supported by the Office of Energy Efficiency and Renewable Energy of the U.S. Department of Energy under Contract No. DE-AC36-08GO28308.

Supporting information for this article is available on the WWW under <http://dx.doi.org/10.1002/anie.201404880>.



Scheme 1. Synthesis of tetrameric cage 4.

**3a** and **3b** in good overall yields. The alkyne metathesis of monomer **3a/3b** (27 mm) was then conducted at 55 °C for 16 h using catalyst **5** (1 mol % per propyne moiety). GPC analysis of the crude product mixture showed the predominant formation of a single species. The metathesis products were isolated in good yields and characterized by 1D  $^1\text{H}$  and  $^{13}\text{C}$  NMR spectroscopy, gCOSY, ROESY, GPC, and MALDI-TOF MS.

As expected, MALDI-TOF MS of the metathesis product ( $\text{R} = \text{C}_3\text{H}_7$ ) showed a strong signal at  $m/z = 1863$  (Supporting Information, Figure S4), which corresponds to a tetramer. However, surprisingly,  $^1\text{H}$  NMR spectrum of the tetramer showed splitting of each set of originally chemically equivalent protons of the monomer unit into two signals in 2:1 ratio (total eight sets of aromatic proton signals). This is inconsistent with the expected highly symmetrical tetrahedral structure **4T<sub>d</sub>** (Figure 1 a), which should show only four sets of

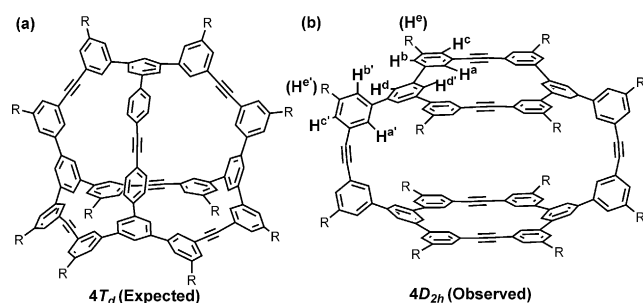


Figure 1. a) Expected structure of tetramer **4T<sub>d</sub>** with  $T_d$  symmetry; b) Observed structure of tetramer **4D<sub>2h</sub>** with  $D_{2h}$  symmetry.

aromatic proton signals. We excluded the possibility of two dimeric cages being interlocked, since 1) the dimeric cage of **3a** (or **3b**) would be highly strained and disfavored; 2) we did not observe any dimer species in the MALDI-MS; and 3) the  $^1\text{H}$  NMR spectra of the cage product at various temperatures consistently show sharp and distinct signals rather than broad and complicated ones. The tetrameric cage **4D<sub>2h</sub>** (Figure 1 b) with  $D_{2h}$  symmetry was then proposed, in which two macrocyclic panels are connected by two diphenylacetylene side arms. This structure gives rise to the splitting of the three arms of a monomer into two types: two identical arms forming the

macrocyclic panel with another monomer and a third arm bridging two macrocycles to form a cage. This agrees with the observed 2:1 ratio of two signals for each set of originally chemically equivalent protons of the monomer unit in  $^1\text{H}$  NMR spectra of **4D<sub>2h</sub>-A4** and **4D<sub>2h</sub>-B4**.

The structure **4D<sub>2h</sub>** was unambiguously determined by single-crystal X-ray diffraction (Figure 2). Needle-like single

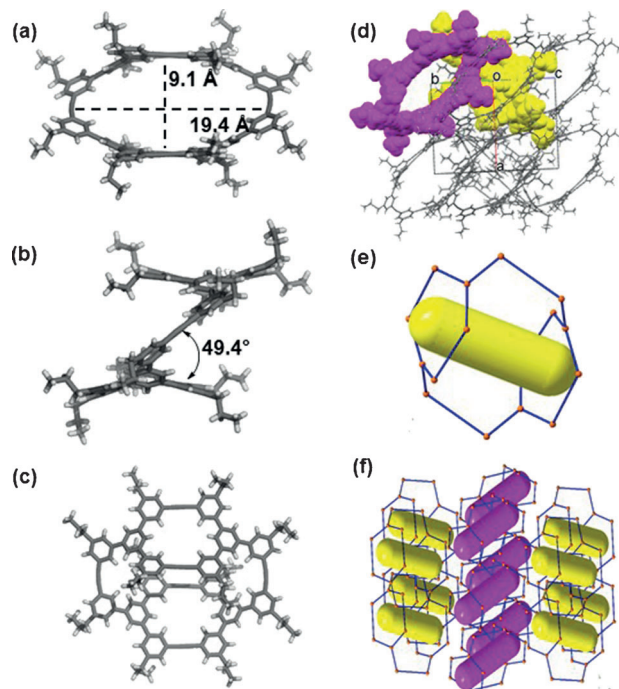
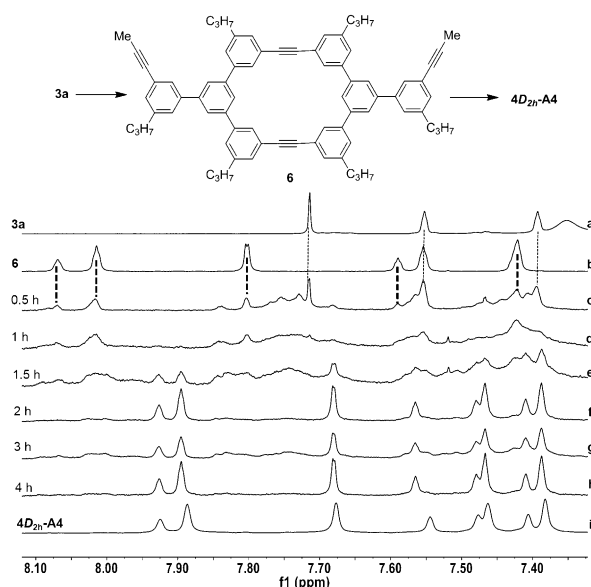


Figure 2. Crystal structure of **4D<sub>2h</sub>-A<sub>4</sub>**: a) Side view 1; b) Side view 2; c) top view; d) crystal packing views along (011) direction; e) simplified view of **4D<sub>2h</sub>-A<sub>4</sub>**; f) simplified view of the crystal packing; the two stacks of the cages oriented differently are color-coded in yellow and magenta. Solvent molecules are omitted for clarity.

crystals of **4D<sub>2h</sub>-A4** were obtained through slow evaporation from a solution of **4D<sub>2h</sub>-A4** in  $\text{CH}_2\text{Cl}_2$  and acetonitrile co-solvent. **4D<sub>2h</sub>-A4** was crystallized in the monoclinic space group  $P12_1/c1$ . It has been a challenge to obtain crystal structures of pure hydrocarbon cages owing to their sensitivity to solvent loss and the easy collapse of the crystals.<sup>[42]</sup> After multiple failed trials, we finally succeeded in determining the structure and packing of the cage **4D<sub>2h</sub>-A4**, albeit with weak X-ray diffraction. The two macrocyclic panels (top and bottom of the cage) are slightly puckered and oriented in a slipped stack fashion relative to each other with the distance of 9.1 Å between them (Figure 2 a,c). Two biphenyl acetylene arms bridge the two panels with the edge-to-face angle of 49.4°, resulting in an overall Z-shape geometry of the cage (Figure 2 b). The dimension of the cage interior at the widest point is 19.4 Å. The packing structure shows that there are two stacks of parallel cages that are arranged at an angle of 141.7° to each other (Figure 2 d,f). There is no connectivity between the cavities of the cages. The interior cavity of each cage is filled with one disordered acetonitrile molecule and two propyl groups from the two neighboring cages. We did not

observe any inter/intramolecular  $\pi$ - $\pi$  interactions. Owing to the absence of functional groups with directing capability, the van der Waals interactions between neighboring molecules and C-H $\cdots$  $\pi$  interactions between the propyl chain and aromatic moieties appear to be the major forces to direct the crystal packing of the cage. This is one of few purely hydrocarbon cage crystal structures.

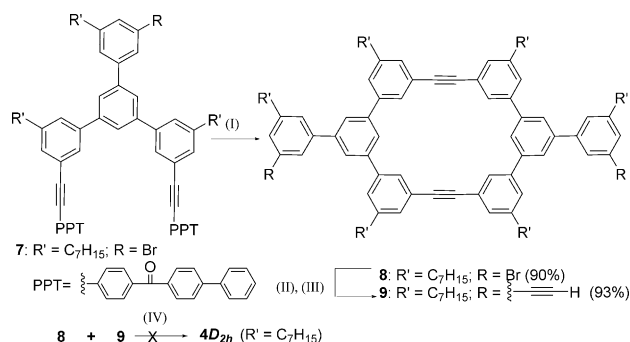
The formation of the cage **4D<sub>2h</sub>** is somewhat surprising, as C<sub>3</sub>-symmetric building blocks generally lead to tetrahedron-shaped structures in the dynamic assembly process through metal coordination or hydrogen bonding.<sup>[43–45]</sup> To gain better understanding of the cage formation process, we monitored the reaction progress. Aliquots of the reaction mixture were withdrawn at different time intervals, and analyzed by GPC and <sup>1</sup>H NMR spectroscopy. The GPC traces showed the initial formation of high molecular weight oligomers and their gradual conversion to **4D<sub>2h</sub>-A4** (Supporting Information, Figure S5). A closer look at the process through <sup>1</sup>H NMR data analysis revealed the initial conversion of monomer **3a** to a substantial amount of macrocycle **6** within 0.5 h (Figure 3). The authentic sample of macrocycle **6** was



**Figure 3.** <sup>1</sup>H NMR spectra of monomer **3a** (a); Authentic sample of macrocyclic intermediate **6** (b); crude mixture after 0.5–4 h (c–h); cage product **4D<sub>2h</sub>-A4** (i). Spectra were recorded in CDCl<sub>3</sub>.

obtained by conducting alkyne metathesis of monomer **3a** in a closed system in the absence of molecular sieves that are typically used to scavenge 2-butyne byproduct. After stirring at 55 °C for 1 h, macrocycle **6** was isolated in 22% yield, together with unreacted monomer **3a**. This experiment supports the notion that the macrocycle **6** is present in a significant amount as a key intermediate during the formation of cage **4D<sub>2h</sub>-A4**. The formation of a tetramer with D<sub>2h</sub> symmetry is therefore likely guided by the initial predominant formation of macrocyclic panels (face-directed) rather than by the geometrical angle of the monomer arms (edge-directed). Intrigued by this observation, we attempted to prepare cage **4D<sub>2h</sub>** (R = n-C<sub>7</sub>H<sub>15</sub>) through kinetically

controlled cross-coupling of two macrocyclic building blocks **8** and **9** (Scheme 2). Macrocyclic **8** was isolated in excellent yield (90%) through alkyne metathesis of compound **7**. This indicates the formation of **8** is a thermodynamically favored



**Scheme 2.** Synthesis of **4D<sub>2h</sub>** by kinetic control. I) cat. **5**, CCl<sub>4</sub>, 55 °C, 90%; II) trimethylsilylacetylene, [Pd(PPh<sub>3</sub>)<sub>2</sub>Cl<sub>2</sub>], CuI, piperidine, THF, 80 °C; III) K<sub>2</sub>CO<sub>3</sub>, MeOH, PhMe, 4 h, RT; IV) Sonogashira cross-coupling reactions under various conditions.

process and no significant angle strain is involved, further supporting the possibility that macrocyclic species **6** forms first and directs the assembly of **4D<sub>2h</sub>**. Complementary macrocyclic building block **9** was then obtained by Sonogashira coupling of **8** with trimethylsilyl acetylene (TMSA) followed by desilylation. Kinetically controlled cross-coupling reactions have played an important role in the construction of well-defined, 2D and 3D molecular architectures.<sup>[37,46,47]</sup> However, the attempted cross-coupling of **8** and **9** failed to yield cage **4D<sub>2h</sub>** under our tested reaction conditions (for details, see the Supporting Information). MALDI-TOF MS, GPC, and <sup>1</sup>H NMR spectroscopy analyses of the crude product mixtures in multiple trials showed the formation of oligomers and polymers without any noticeable amount of the cage products. More exotic reaction conditions that might lead to the desired cage formation were not further explored.

To confirm that the formation of cage **4D<sub>2h</sub>** is a dynamic and reversible process, we conducted the scrambling experiment between **4D<sub>2h</sub>-A4** and **4D<sub>2h</sub>-B4**. A 1:2 mixture of **4D<sub>2h</sub>-A4** and **4D<sub>2h</sub>-B4** were subjected to alkyne metathesis (55 °C, CCl<sub>4</sub>, 16 h). The GPC trace of the crude reaction mixture showed a new peak with a broad shoulder (Figure 4). MALDI-MS of the crude reaction mixture showed all possible scrambled products, **A3B**, **A2B2**, **AB3** together with **A4** and **B4**, indicating that the system is dynamic and the cage **4D<sub>2h</sub>** is not kinetically trapped.

The cage **4D<sub>2h</sub>-A4** has a large cavity, with a distance between the top and bottom panels of about 9.0 Å based on the crystal structure. The shape-persistency and the rigid backbones consisting of aromatic moieties make cage **4D<sub>2h</sub>-A4** an attractive host for guest molecules, such as fullerenes. To investigate the host-guest binding interactions between **4D<sub>2h</sub>-A4** and C<sub>60</sub> or C<sub>70</sub>, we conducted <sup>1</sup>H NMR titration experiments at 298 K in [D<sub>8</sub>]toluene. Interestingly, **4D<sub>2h</sub>-A4** showed a very weak binding interaction with C<sub>60</sub> according to the <sup>1</sup>H NMR data obtained from the titration experiment. We did not observe any significant chemical shift changes of the

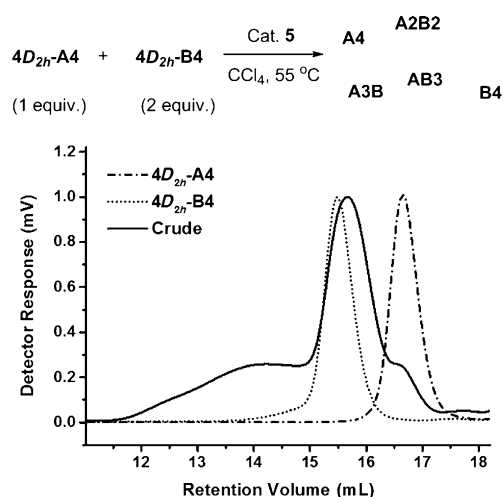


**Figure 4.** The GPC traces (normalized) of  $4D_{2h}$ -A4,  $4D_{2h}$ -B, and the crude mixture of the scrambling experiment.

cage protons when the solution of  $4D_{2h}$ -A4 in toluene was titrated with increasing amount of  $C_{60}$  up to 6.2 equiv (Supporting Information, Figure S9). In contrast, the binding interaction between  $4D_{2h}$ -A4 and  $C_{70}$  was evident. The addition of  $C_{70}$  (0–8.6 equiv) to the solution of  $4D_{2h}$ -A4 in toluene induced significant chemical shift changes of the aromatic and aliphatic protons that are in the close proximity to the fullerene guest (Figure 5 a). The protons  $H^a$ ,  $H^a'$ , and  $H^d$

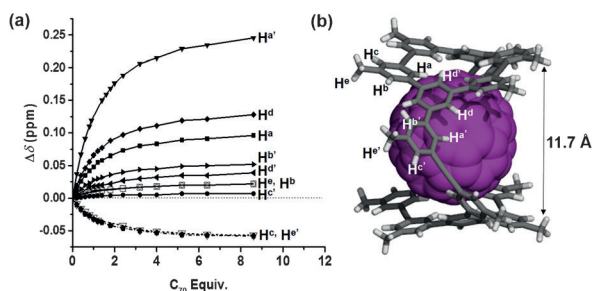


**Figure 5.** a) The chemical-shift changes in  $^1H$  NMR spectra obtained during the titration of  $4D_{2h}$ -A4 (0.14 mM) with an increasing amount of  $C_{70}$  (0–8.6 equiv). b) The computational model (side view) of  $C_{70}@4D_{2h}$ -A4; methyl groups are used for simplification. The NMR titrations were conducted in  $[D_8]$ toluene.

point toward the cavity and show pronounced upfield shifts upon fullerene binding. The  $H^d$  protons that are located at the inner side of the macrocyclic rings are pushed away from the cavity as the result of the puckered shape of the macrocycles, leading to the small upfield shift of  $H^d$  signals upon fullerene binding. Aromatic proton  $H^b$  and the methylene protons ( $H^c$ ) are shielded in the presence binding of the fullerene guest.

Analysis of the Job Plot (Supporting Information, Figure S9) shows 1:1 stoichiometry between  $C_{70}$  and the cage  $4D_{2h}$ -A4 with the binding constant of  $3.9 \times 10^3 \text{ L mol}^{-1}$ . The energy-minimized structure of  $C_{70}@4D_{2h}$ -A4 shows that upon fullerene binding the bottom and top macrocyclic panels become perfectly co-facial rather than the original “slipped” conformation of the empty cage, with an enlarged interpanel

distance about 11.7 Å (Figure 5b). Based on the computer modeling, the binding energy of  $4D_{2h}$ -A4 with  $C_{70}$  is 10 kcal mol $^{-1}$  lower than that of binding with  $C_{60}$  (–48.7 vs. –38.4 kcal mol $^{-1}$ ). Presumably  $C_{70}$  is bigger and more ellipsoidal than  $C_{60}$ , and resembles the shape of the cavity, thus providing a better fit inside the cage and a stronger binding interaction.

In conclusion, tetrameric cages  $4D_{2h}$  with an uncommon  $D_{2h}$  symmetry were obtained through one-step alkyne metathesis from readily accessible  $C_3$ -symmetrical propynyl-substituted monomers in good yields. The structure of the cage  $4D_{2h}$ -A4 was fully characterized by 1D  $^1H$  and  $^{13}C$  NMR spectroscopy, gCOSY, ROESY, GPC, MALDI-TOF MS, and single-crystal X-ray diffraction. The formation of the cage is likely a face-directed dynamic assembly process, which involves the formation of dimeric macrocycle panels as the key intermediates. Our attempts to synthesize the cage  $4D_{2h}$  through cross-coupling of two macrocyclic building blocks under various reaction conditions failed, showing that a dynamic covalent approach could be advantageous compared to kinetically controlled approaches for constructing complex molecular architectures. Finally, the cage  $4D_{2h}$ -A4 shows selective binding interactions for  $C_{70}$  ( $K = 3.9 \times 10^3 \text{ L mol}^{-1}$ ) over  $C_{60}$  (no noticeable binding).

### Experimental Section

X-ray intensity data were collected on a Bruker D8 VENTURE diffractometer system equipped with a multilayer mirror monochromator and a Cu  $K_{\alpha}$  microfocus sealed tube ( $\lambda = 1.54178 \text{ \AA}$ ). The structure was solved and refined using the Bruker SHELXTL Software Package.  $4D_{2h}$ -A4:  $C_{155.20}H_{149.80}Cl_4N_{4.60}$ , 0.032 mm  $\times$  0.117 mm  $\times$  0.159 mm, space group  $P12_1/c1$ ,  $Z = 2$ ;  $\rho$  1.100 g cm $^{-3}$ ,  $F(000)$  2362 e $^{-}$ . The final anisotropic full-matrix least-squares refinement on  $F^2$  (765 variables) converged at  $R1 = 11.39\%$  (observed data),  $wR2 = 38.15\%$  (all data). Goodness-of-fit 1.785; largest peak/hole in the final difference electron density synthesis 1.234 e $^{-}$   $\text{\AA}^{-3}$ /–1.128 e $^{-}$   $\text{\AA}^{-3}$  with an RMS deviation of 0.121 e $^{-}$   $\text{\AA}^{-3}$ . CCDC 999558 contains the supplementary crystallographic data for this paper. These data can be obtained free of charge from The Cambridge Crystallographic Data Centre via [www.ccdc.cam.ac.uk/data\\_request/cif](http://www.ccdc.cam.ac.uk/data_request/cif).

Received: May 1, 2014

Revised: June 7, 2014

Published online: August 21, 2014

**Keywords:** alkyne metathesis · dynamic covalent assembly · fullerene receptors · organic molecular cages · thermodynamic control

- [1] J. Tian, P. K. Thallapally, B. P. McGrail, *CrystEngComm* **2012**, *14*, 1909–1919.
- [2] A. I. Cooper, *Angew. Chem.* **2011**, *123*, 1028–1030; *Angew. Chem. Int. Ed.* **2011**, *50*, 996–998.
- [3] Y. Jin, Y. Zhu, W. Zhang, *CrystEngComm* **2013**, *15*, 1484–1499.
- [4] T. Mitra, K. E. Jelfs, M. Schmidtman, A. Ahmed, S. Y. Chong, D. J. Adams, A. I. Cooper, *Nat. Chem.* **2013**, *5*, 276–281.
- [5] C. Schouwey, R. Scopelliti, K. Severin, *Chem. Eur. J.* **2013**, *19*, 6274–6281.

- [6] C. X. Zhang, Q. Wang, H. Long, W. Zhang, *J. Am. Chem. Soc.* **2011**, *133*, 20995–21001.
- [7] R. McCaffrey, H. Long, Y. Jin, A. Sanders, W. Park, W. Zhang, *J. Am. Chem. Soc.* **2014**, *136*, 1782–1785.
- [8] Z. H. Lin, J. L. Sun, B. Efremovska, R. Warmuth, *Chem. Eur. J.* **2012**, *18*, 12864–12872.
- [9] S. J. Rowan, S. J. Cantrill, G. R. L. Cousins, J. K. M. Sanders, J. F. Stoddart, *Angew. Chem.* **2002**, *114*, 938–993; *Angew. Chem. Int. Ed.* **2002**, *41*, 898–952.
- [10] P. T. Corbett, J. Leclaire, L. Vial, K. R. West, J. L. Wietor, J. K. M. Sanders, S. Otto, *Chem. Rev.* **2006**, *106*, 3652–3711.
- [11] M. E. Belowich, J. F. Stoddart, *Chem. Soc. Rev.* **2012**, *41*, 2003–2024.
- [12] Y. Jin, C. Yu, R. J. Denman, W. Zhang, *Chem. Soc. Rev.* **2013**, *42*, 6634–6654.
- [13] Y. Jin, Q. Wang, P. Taynton, W. Zhang, *Acc. Chem. Res.* **2014**, *47*, 1575–1586.
- [14] N. M. Rue, J. L. Sun, R. Warmuth, *Isr. J. Chem.* **2011**, *51*, 743–768.
- [15] K. Severin, *Dalton Trans.* **2009**, 5254–5264.
- [16] R. Nishiyabu, Y. Kubo, T. D. James, J. S. Fossey, *Chem. Commun.* **2011**, *47*, 1124–1150.
- [17] A. C. Dash, B. Dash, S. Praharaaj, *J. Chem. Soc. Dalton* **1981**, 2063–2069.
- [18] J. Xu, D. Duran, B. Mao, *J. Liq. Chromatogr. Relat. Technol.* **2006**, *29*, 2795–2806.
- [19] J. S. Moore, *Acc. Chem. Res.* **1997**, *30*, 402–413.
- [20] Y. Tobe, M. Sonoda, *Modern Cyclophane Chemistry*, Wiley-VCH, Weinheim, **2004**, pp. 1–40.
- [21] A. Avellaneda, P. Valente, A. Burgun, J. D. Evans, A. W. Markwell-Heys, D. Rankine, D. J. Nielsen, M. R. Hill, C. J. Sumbly, C. J. Doonan, *Angew. Chem.* **2013**, *125*, 3834–3837; *Angew. Chem. Int. Ed.* **2013**, *52*, 3746–3749.
- [22] C. Zhang, C. F. Chen, *J. Org. Chem.* **2007**, *72*, 9339–9341.
- [23] H. L. Andersson, G. Gil-Ramirez, S. D. Karlen, A. Shundo, K. Porfyraakis, Y. Ito, G. A. D. Briggs, J. J. L. Morton, *Org. Lett.* **2010**, *12*, 3544–3547.
- [24] M. J. Langton, J. D. Matichak, A. L. Thompson, H. L. Anderson, *Chem. Sci.* **2011**, *2*, 1897–1901.
- [25] M. C. O'Sullivan, J. K. Sprafke, D. V. Kondratuk, C. Rinfray, T. D. W. Claridge, A. Saywell, M. O. Blunt, J. N. O'Shea, P. H. Beton, M. Malfois, H. L. Anderson, *Nature* **2011**, *469*, 72–75.
- [26] Y. Sato, R. Yamasaki, S. Saito, *Angew. Chem.* **2009**, *121*, 512–515; *Angew. Chem. Int. Ed.* **2009**, *48*, 504–507.
- [27] R. R. Schrock, C. Czekelius, *Adv. Synth. Catal.* **2007**, *349*, 55–77.
- [28] A. Fürstner, *Angew. Chem.* **2013**, *125*, 2860–2887; *Angew. Chem. Int. Ed.* **2013**, *52*, 2794–2819.
- [29] X. A. Wu, M. Tamm, *Beilstein J. Org. Chem.* **2011**, *7*, 82–93.
- [30] K. Jyothish, W. Zhang, *Angew. Chem.* **2011**, *123*, 8628–8630; *Angew. Chem. Int. Ed.* **2011**, *50*, 8478–8480.
- [31] A. Mortreux, M. Blanchar, *J. Chem. Soc. Chem. Commun.* **1974**, 786–787.
- [32] D. Villemin, M. Héroux, V. Blot, *Tetrahedron Lett.* **2001**, *42*, 3701–3703.
- [33] V. Huc, R. Weihofen, I. Martin-Jimenez, P. Oulie, C. Lepetit, G. Lavigne, R. Chauvin, *New J. Chem.* **2003**, *27*, 1412–1414.
- [34] V. Maraval, C. Lepetit, A.-M. Caminade, J.-P. Majoral, R. Chauvin, *Tetrahedron Lett.* **2006**, *47*, 2155–2159.
- [35] S. Lysenko, B. Haberlag, C. G. Daniliuc, P. G. Jones, M. Tamm, *ChemCatChem* **2011**, *3*, 115–118.
- [36] A. Fürstner, K. Grela, *Angew. Chem.* **2000**, *112*, 1292–1294; *Angew. Chem. Int. Ed.* **2000**, *39*, 1234–1236.
- [37] W. Zhang, J. S. Moore, *Angew. Chem.* **2006**, *118*, 4524–4548; *Angew. Chem. Int. Ed.* **2006**, *45*, 4416–4439.
- [38] U. H. F. Bunz, *Acc. Chem. Res.* **2001**, *34*, 998–1010.
- [39] H. Yang, Y. Jin, Y. Du, W. Zhang, *J. Mater. Chem. A* **2014**, *2*, 5986–5993.
- [40] D. W. Paley, D. F. Sedbrook, J. Decatur, F. R. Fischer, M. L. Steigerwald, C. Nuckolls, *Angew. Chem.* **2013**, *125*, 4689–4692; *Angew. Chem. Int. Ed.* **2013**, *52*, 4591–4594.
- [41] H. Yang, Z. Liu, W. Zhang, *Adv. Synth. Catal.* **2013**, *355*, 885–890.
- [42] Z. Y. Wu, S. Lee, J. S. Moore, *J. Am. Chem. Soc.* **1992**, *114*, 8730–8732.
- [43] Y. Inokuma, S. Yoshioka, M. Fujita, *Angew. Chem.* **2010**, *122*, 9096–9098; *Angew. Chem. Int. Ed.* **2010**, *49*, 8912–8914.
- [44] S. R. Seidel, P. J. Stang, *Acc. Chem. Res.* **2002**, *35*, 972–983.
- [45] M. Yoshizawa, J. K. Klosterman, M. Fujita, *Angew. Chem.* **2009**, *121*, 3470–3490; *Angew. Chem. Int. Ed.* **2009**, *48*, 3418–3438.
- [46] C. Grave, A. D. Schluter, *Eur. J. Org. Chem.* **2002**, 3075–3098.
- [47] M. Iyoda, J. Yamakawa, M. J. Rahman, *Angew. Chem.* **2011**, *123*, 10708–10740; *Angew. Chem. Int. Ed.* **2011**, *50*, 10522–10553.